ICES Journal of
Marine Science

Original Article

Acoustic biomass estimation of mesopelagic fish: backscattering from individuals, populations, and communities

Peter C. Davison[1]*, J. Anthony Koslow[2], and Rudy J. Kloser[3]

[1]*Farallon Institute for Advanced Ecosystem Research, Petaluma, CA 94952, USA*
[2]*Scripps Institution of Oceanography, University of California at San Diego, 9500 Gilman Drive, La Jolla, CA 92093-0218, USA*
[3]*CSIRO Oceans and Atmosphere Flagship, GPO Box 1538, Hobart, TAS 7001, Australia*

Corresponding author: tel/fax: +1 707 981 8033; e-mail: pdavison@ucsd.edu

Acoustic survey methods are useful to estimate the distribution, abundance, and biomass of mesopelagic fish, a key component of open ocean ecosystems. However, mesopelagic fish pose several challenges for acoustic biomass estimation based on their small size, wide depth range, mixed aggregations, and length-dependent acoustic reflectance, which differentiate them from the larger epipelagic and neritic fish for which these methods were developed. Foremost, there is a strong effect of depth on swimbladder resonance, so acoustic surveys of mesopelagic fish must incorporate depth-stratification. Additionally, the 1–3 cm juveniles of many species are not only more abundant, but can also be stronger acoustic backscatterers than the larger adults that comprise most of the biomass. The dominant species in terms of biomass may thus be weak acoustic backscatters. Failure to properly incorporate depth, the full size distribution, and certain less-abundant species into mesopelagic acoustic analyses could lead to errors in estimated biomass of up to three orders of magnitude. Thus, thorough validation, or "ground-truthing", of the species composition, depth structure, population size distribution, capture efficiency of the sampling device, and acoustic properties of the fish present is critical for credible acoustic estimates of mesopelagic fish biomass. This is not insurmountable, but requires more ancillary data than is usually collected.

Keywords: acoustic backscatter, biomass assessment, mesopelagic fish, resonance, swimbladder, target strength.

Introduction

Mesopelagic fish are virtually ubiquitous in the world's oceans, being found in all oceans except the Arctic (Gjosaeter and Kawaguchi, 1980). In most of the ocean, they appear the dominant zooplankton consumers, so they play a key role in marine foodwebs (Mann, 1984; Pakhomov et al., 1996; Gartner et al., 1997). They reside at mesopelagic depths ($\sim$200–1000 m) in daylight, where they help form the acoustic deep scattering layer (DSL). Many ascend to feed in near-surface waters at night, and return to depth before dawn in a diel vertical migration (DVM). They thus link epipelagic and deep-water food chains and by transporting considerable zooplankton production to the deep ocean, may play a key role in biogeochemical cycling and carbon sequestration (Davison et al., 2013; Irigoien et al., 2014). Their biomass is therefore a critical parameter for global and regional models of marine ecosystems and

biogeochemistry. However, at present, there remain approximately order of magnitude uncertainties with regard to their biomass both globally and regionally (Irigoien et al., 2014).

Gjosaeter and Kawaguchi (GK; 1980) estimated the global biomass of mesopelagic fish was $\sim$1 billion t, based on a review of global mesopelagic sampling programmes to date. They relied on micronekton net sampling for their biomass estimates, which generally ranged between 1 and 5 g m^{-2}. Since publication of GK's landmark study, there is increased evidence from studies based on combining acoustics with trawling that escapement and avoidance from pelagic trawls leads to underestimation by trawls of a factor of 7 or more (Koslow et al., 1997; Kloser et al., 2009; Yasuma and Yamamura, 2010; Davison, 2011b). Substantial avoidance of pelagic trawls has also been directly observed (Kaartvedt et al., 2012). Thus, acoustic estimates of biomass generally, but not

always, exceed those from trawls (Koslow *et al.*, 1997; Kloser *et al.*, 2009; Kaartvedt *et al.*, 2012; Davison *et al.*, 2015). Trawl biomass may exceed acoustic estimates due to patchiness or when the dominant species for biomass is a weak scatterer (Davison *et al.*, 2015).

No single correction for capture efficiency can be generally applied, because it is influenced by the size and swimming ability of the fish, mesh size, tow speed, mouth diameter, and net design. Thus, large trawls with large meshes likely reduce avoidance but increase escapement through the meshes, thereby preferentially sampling the larger size fraction of the micronekton community. Smaller nets with finer meshes reduce escapement but suffer enhanced avoidance, leading to a reduced size frequency distribution of the sampled community. Given that trawl samples are often used to ground-truth the size and species composition of an ensonified assemblage, the issues of potential bias are readily apparent.

There are a range of issues related uniquely to the use of acoustics to assess mesopelagic fish biomass. Foremost is the issue of resonance by gas-filled swimbladders, which is a non-linear function of depth, the size of the gas bubble, membrane properties, and acoustic frequency. For mesopelagic fish, resonance at frequencies $\leq$38 kHz is particularly pronounced (Kloser *et al.*, 2002; Godo *et al.*, 2009). Complicating the issue, swimbladder morphology and inflation can vary ontogenetically in midwater fish (Butler and Pearcy, 1972; Davison, 2011a). Swimbladder volume and target strength (*TS*) also vary with depth, which may change on a diel basis due to vertical migration (Hersey *et al.*, 1962; Godo *et al.*, 2009).

To compound these issues, fish are not the only organisms with gas-filled organs at midwater depths. Physonect and some cystonect siphonophores possess pneumatophores for buoyancy and may be highly abundant at midwater depths (Barham, 1963; Robison *et al.*, 1998). Unfortunately, although these siphonophores may be regionally dominant organisms, they are fragile and poorly sampled by trawls. In general, their abundance in midwater ecosystems is unknown, and their high acoustic reflectance may lead to overestimates in midwater fish biomass estimates if their backscattering is subsumed with that of the fish.

Irigoien *et al.* (2014) recently used 38 kHz acoustic data obtained during a circumglobal voyage without accompanying trawl data to estimate the global biomass of mesopelagic fish, an estimate of great ecological importance. Irigoien *et al.* (2014) acknowledged that their result had considerable uncertainty—an order of magnitude and possibly more. Their study, which by necessity ignored many of the caveats outlined above, has led us to examine the limits of current acoustic methods of biomass estimation for mesopelagic fish. In this paper, we use trawl and acoustic data from cruises in the California Current ecosystem (CCE) and North Pacific subtropical gyre (NPSG) to highlight the problems in the application of traditional acoustic survey methods to mesopelagic fish, and also to point to the methods required to narrow uncertainty to more acceptable levels. We use only daylight acoustic data only to minimize complication from DVM behaviour. These data are typical for the CCE and NPSG, but are not regionally representative, and thus we present the results as examples but not estimates of the CCE and NPSG mesopelagic fish abundance.

Methods
Fish collection

A total of 125 oblique trawls to depths >400 m were made over the course of nine cruises (CCE-P0704, CCE-P0810, ORCAWALE 2008,

SEAPLEX, and CalCOFI cruises 1008, 1011, 1108, 1110, and 1202) in the CCE and NPSG from 2007 to 2012 using a 5-m^2 Matsuda-Oozeki-Hu trawl (MOHT; Oozeki *et al.*, 2004) or 3-m^2 Isaacs–Kidd midwater trawl (IKMT; Isaacs and Kidd, 1953) fitted with a constant 1.7 mm mesh (Figure 1). Water flow through the trawl mouth was measured with a TSK flowmeter for the MOHT and calculated from ship speed for the IKMT. Standard length (L_s) was measured to the nearest millimetre and blotted wet weight (W_w) measured to a precision of 0.01 g or estimated from $W_w(L_s)$ regressions (Figure 2). Abundance and biomass were estimated by dividing the number and weight (respectively) of captured fish by the volume of water filtered, and then multiplying by the depth of the trawl.

Three model species of mesopelagic fish in the CCE were chosen for study of acoustic backscattering. *Diaphus theta*, *Stenobrachius leucopsarus*, and *Leuroglossus stilbius* are the most abundant vertically migratory species in our collections from the CCE with gas-filled swimbladders, regressed swimbladders as adults, and no swimbladder, respectively (Davison, 2011a). All individuals of these species collected from 122 deep trawls in the CCE (Figure 1) were pooled to estimate the length and weight distributions of their populations. Catches were pooled because the distribution of mesopelagic fish is patchy, catches of individual species from single trawls are often low, and the larger size classes are relatively rare. Both IKMT and MOHT trawls were used to collect fish of the model species, and abundance was corrected for gear differences (MOHT catch is 2.1 times that of the IKMT; Yamamura *et al.*, 2010; Davison *et al.*, 2013) before pooling. For community-level comparisons, the entire normalized catch from a station in the CCE (four trawls from CCE-P0810 cruise, "Cycle 3") was compared with that from a station in the NPSG (three trawls from SEAPLEX cruise, "Station 2"; Figure 1). Only MOHT trawls were used at the CCE and NPSG stations. We use the word "community" here and hereafter in the sense of the species present at our two stations, and their size distribution. These stations may or may not be representative of broader time or space scales.
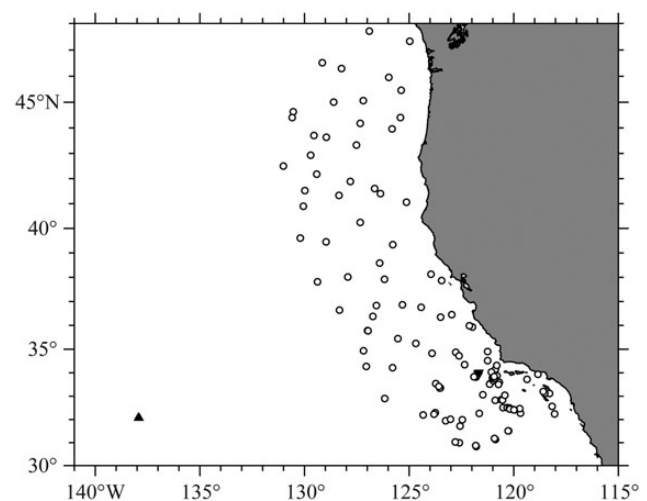
Figure 1. Trawl locations. Individuals of *D. theta*, *S. leucopsarus*, and *L. stilbius* were taken from locations marked by open circles. The full fish community was studied at one site in each of two ecosystems; the North Pacific subtropical gyre (upward filled triangle; three trawls), and the California Current ecosystem (downward facing triangle; four trawls).
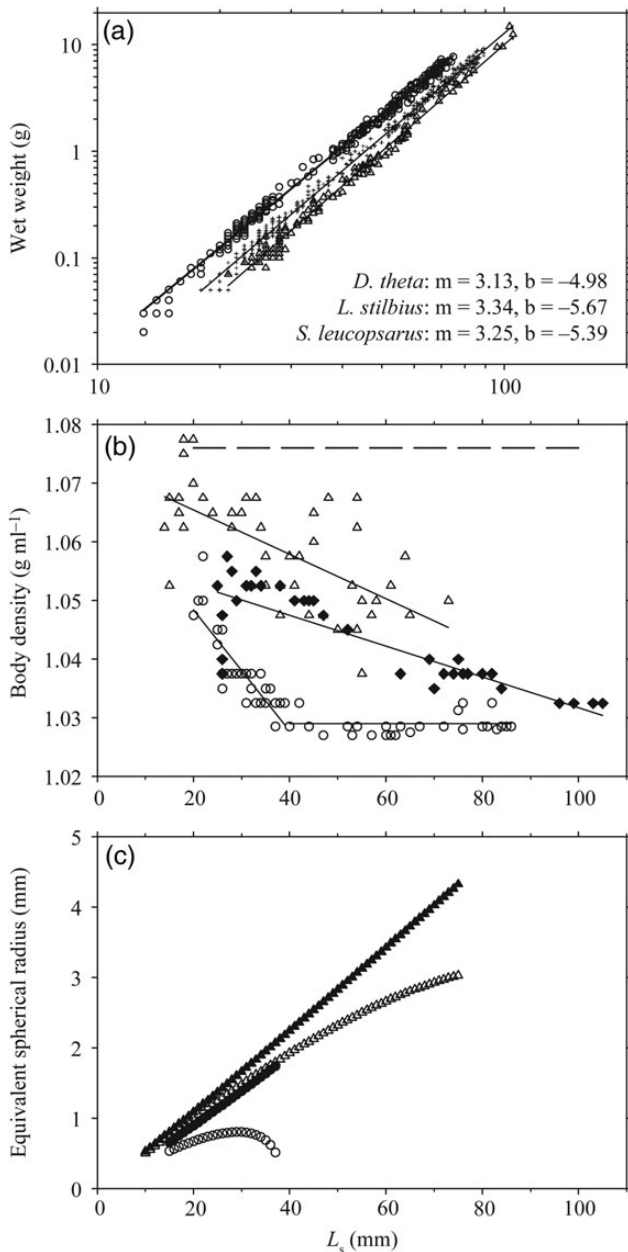
Figure 2. L_s-dependent parameters for the model species: (a) W_w for *D. theta* (circles), *S. leucopsarus* (crosses), and *L. stilbius* (triangles) with regression slopes ("*m*") and intercepts ("*b*"); (b) body density for *S. leucopsarus* (open circles), *D. theta* (open triangles), and *L. stilbius* (closed diamonds) with typical epipelagic fish density (1.076) shown as a dashed line; and (c) ESR of the swimbladders of *D. theta* (closed triangle for constant body density of 1.076 g ml^{-1}, open triangle for measured body density), and *S. leucopsarus* (closed circle for constant body density of 1.076 g ml^{-1}, open circle for measured body density).

Forward acoustic modelling of fish

Backscattering from fish was estimated at two depths, 300 and 600 m, with acoustic "forward" models of individual fish. Acoustic backscattering from a fish body was assumed to be the same as that from a fluid-filled cylinder (Stanton, 1988) of the same length, volume, and density as the fish. Backscattering from gas within the swimbladder was estimated as that from a sphere

using the Johnson (1977) high-pass model for $ka < 0.15$ (Rayleigh region and primary resonance) and the Anderson (1950) model for $ka \geq 0.15$ (geometric region), where k is the wave number and a the equivalent spherical radius (ESR). The volume of gas within the swimbladder was estimated as that required for neutral buoyancy. High-frequency resonance in the sphere model was smoothed by averaging the modelled backscattering over ten iterations in which gas volume varied slightly (normal distribution with s.d. = 0.2% of the calculated gas volume). Fish W_w as a function of L_s, body density, and length-dependent swimbladder inflation followed Davison (2011a) and Davison *et al.* (2015). Temperature and salinity profiles were measured with a Sea-Bird SBE 911plus CTD. Water temperature at the NPSG station was 9.7 and 5.2°C for 300 and 600 m depths, respectively. Salinity was 34.0 psu at both depths. At the CCE station, temperature was 7.6 and 5.2°C at 300 and 600 m depths, respectively. Salinity was 34.1 psu at both depths. The density of water was calculated following Millero *et al.* (1980). The speed of sound in seawater, c, was calculated based upon the pressure, temperature, and salinity at 50 m depth per Mackenzie (1981). The acoustic backscattering cross sections (σ_{bs}) of the modelled body and gas were added to form the overall σ_{bs} of the fish. TS (dB re 1 m^2) is the decibel form of the σ_{bs} (m^2), and the two variables are related by the equation $TS = 10\log_{10}(\sigma_{bs})$.

EK60

Multifrequency volume backscattering strength (S_v; dB re m^{-1}) data were collected at the CCE and NPSG stations using Simrad EK60 split-beam echosounders, although only 38 kHz was used for echo integration here. The EK60's were calibrated for each cruise using the standard sphere method (Foote *et al.*, 1987). Pulse length was set to 0.512 ms for the CCE and 1.024 ms for the NPSG station. Ping rate was 0.5 s^{-1} for the CCE and 0.25 s^{-1} for the NPSG station. Thirty-eight kilohertz beam angles were 7° for the NPSG transducer and 12° for the CCE transducer. Power for the 38 kHz transducer was 1 kW for the CCE and 2 kW for the NPSG station.

The technique of echo integration to estimate the abundance of fish requires a mean σ_{bs} (m^2) in combination with echograms of volume backscattering coefficient (s_v; m^{-1}), the linear form of volume backscattering strength [$S_v = 10\log_{10}(s_v)$; dB re 1 m^{-1}; MacLennan *et al.*, 2002]. s_v is integrated by depth to produce the area backscattering coefficient, s_a (m^2 m^{-2}), and abundance = s_a/σ_{bs} (ind. m^{-2}; Simmonds and MacLennan, 2005). Biomass (g m^{-2}) is simply abundance multiplied by the mean W_w (g). Daylight acoustic data from ~150 min during the second and first deep trawls in the CCE and NPSG, respectively, were processed and noise removed using Echoview software following De Robertis and Higginbottom (2007). S_v was integrated over depth and then averaged over time for each echogram to produce a depth vector of s_a at each station that was used for echo integration.

Capture efficiency assumption

Larger fish are known to be stronger swimmers, and thus better able to avoid a net (Gartner *et al.*, 1989; Itaya *et al.*, 2007). This length-dependence of avoidance ability can bias the length distribution of a trawl catch with respect to that present in the sampled water, and thus bias the models of backscattering used to interpret acoustic data (Davison *et al.*, 2015). We applied a correction factor to capture efficiency to evaluate the effect of L_s-dependent avoidance on acoustic and trawl estimates of biomass. With this assumption of "differential capture efficiency", capture efficiency was assumed to

decrease with increasing L_s: 100% for $L_s \leq 10$ mm, decreasing 1% mm^{-1} for $10 < L_s < 105$ mm, and 5% for $L_s \geq 105$ mm. Although the precise functional form of the relationship between L_s and capture efficiency is unknown, capture efficiency has been shown to decrease linearly with L_s for a myctophid species (Itaya *et al.*, 2007) and anchovy larvae (Murphy and Clutter, 1972).

Results

Model species

A total of 1646 *D. theta* (L_s 11–75 mm), 6886 *S. leucopsarus* (L_s 15–105 mm), and 245 *L. stilbius* (L_s 16–84 mm) were collected throughout the CCE (Figure 1). *Diaphus theta* has an inflated swim-bladder throughout its length range, although body density decreases with increasing L_s (Figure 2; Davison, 2011a). *Stenobrachius leucopsarus* has a regressed swimbladder as an adult, with gas lost at $L_s = \sim 40$ mm, coinciding with an inflection point in the slope of body density with L_s (Figure 2; Davison, 2011a). *Stenobrachius leucopsarus* of $L_s > 40$ mm are almost neutrally buoyant in seawater without gas. *Leuroglossus stilbius* never possesses a gas-filled swimbladder, and its body density also decreases with increasing L_s (Figure 2). For purposes of buoyancy calculation and acoustic modelling, fish are commonly assumed to have a body density of ~ 1.076 g ml^{-1}, a typical value for an epipelagic fish (Saenger, 1989; Clay and Horne, 1994; Davison, 2011a). Mesopelagic fish generally have a lower body density than 1.076 g ml^{-1}, often much lower (Figure 2b), and thus require a smaller volume of gas to maintain buoyancy than an epipelagic fish. The volume of gas required for buoyancy, expressed as an ESR, diverges progressively from that of an epipelagic fish with increasing L_s (Figure 2c).

CCE and NPSG stations

A total of 1517 non-larval fish belonging to 33 species were captured in four deep trawls at the CCE station. The mean W_w was 0.8 g, although the mode was 0.12 g (Figure 3). The modal W_w corresponded to an *S. leucopsarus* of ~ 23 mm L_s (Figures 2 and 3). Abundance was dominated by *Cyclothone* spp. (59%), and biomass was dominated by lanternfish (64%). Four species of *Cyclothone* are present in the CCE, but two species dominate abundance; *Cyclothone signata* and *Cyclothone acclinidens*. *Cyclothone signata* has an inflated swimbladder, but *C. acclinidens* does not. Both species are small (L_s 2–3.6 and 2–6 cm, respectively), and can be expected to scatter sound similarly to *S. leucopsarus* and *L. stilbius* of the same L_s. *Stenobrachius leucopsarus* was the most common lanternfish species, followed by *D. theta*. At the CCE station, fish with gas-filled swimbladders outnumbered those without inflated swimbladders for $W_w < 1$ g (69%; Figure 3), but formed a minority of fish with $W_w > 1$ g (43%; Figure 3). The overall abundance fraction of fish with gas-filled swimbladders was 58%.

At the NPSG station, 1054 non-larval fish from 50 species were captured in the three deep trawls. Overall abundance was similar to the CCE station but biomass was lower (Table 1). Both abundance and biomass were dominated by *Cyclothone* spp. (66 and 45%, respectively). The most abundant species was *C. signata*, whereas the dominant species for biomass was *Cyclothone atraria*. The mode of the W_w distribution was the same at both stations (0.12 g; Figure 3), but the mean W_w was lower in the NPSG (0.2 g). Fish with gas-filled swimbladders comprised a majority of abundance in all weight classes save 0.64–2.56 g, although the dominant species by biomass (*C. atraria*) does not have an inflated swimbladder and can be expected
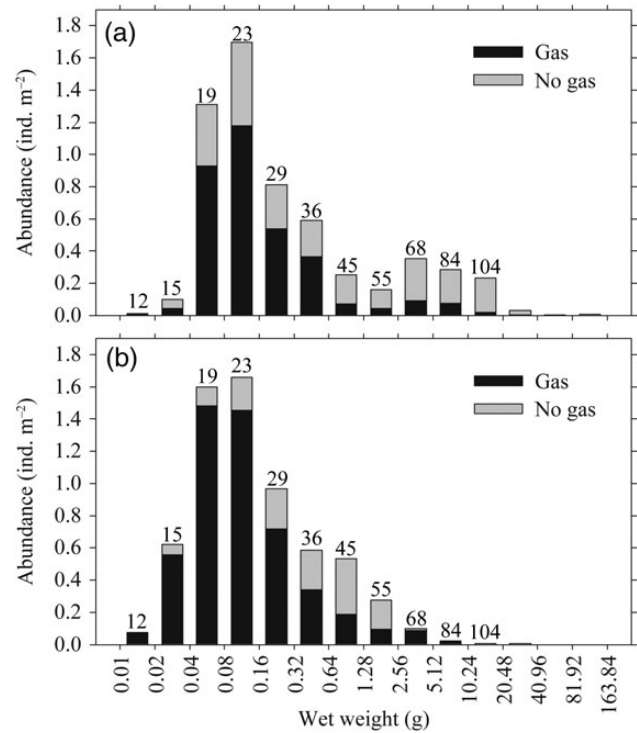
Figure 3. W_w distribution at the (a) CCE and (b) NPSG stations. Note doubling scale of *x*-axis weight bins. *x*-axis labels are the weight boundaries for the intermediate bars. The median *S. leucopsarus* L_s (mm) corresponding to W_w bins are given above each bar.

to scatter sound similarly to *L. stilbius*. The overall abundance fraction of fish with inflated swimbladders at the NPSG station was 78%.

The 38 kHz daytime DSL was at 200–550 m depth at the CCE station and at 450–750 m at the NPSG station (Figure 4). At both stations, 200–750 m area backscattering strength [$S_a = 10\log_{10}(s_a)$] was similar, −45.2 and −45.5 dB re 1 m^2 m^{-2} at the CCE and NPSG stations, respectively.

Individual frequency spectra

The frequency spectra of individual fish vary with size, depth, and body density. Body density acts on acoustic backscattering in two ways, directly through the density contrast with the surrounding water, and indirectly through the volume of gas required for neutral buoyancy. Increased body density (increased ESR of swimbladder gas) lowers the primary resonance frequency, increases geometric region backscattering from the swimbladder, and increases backscattering from the fish body (Figure 5). ESR generally, but not always, increases with increasing L_s (Figure 2), and thus large fish with gas-filled swimbladders scatter more sound than (non-resonant) smaller ones (Figure 5). However, the resonant frequency is higher for smaller radii, and at the study frequency (38 kHz), the smallest fish have similar *TS* to the largest ones (Figure 5). Increasing pressure (depth) increases the density and hence the resonant frequency of the gas in a swimbladder. Thus, the same small fish may be non-resonant and weakly scattering at a depth of 300 m, but resonant and scatter tenfold more sound at a depth of 600 m, or *vice versa* (Figure 5). Differences between a real fish and the simple geometric shapes modelled here will strongly affect the location and magnitude of high-frequency resonances and nulls (Figure 5).

Most of the high-frequency structure is at frequencies >38 kHz, and thus, our simple models are suited for our study frequency.

Length dependence of backscattering

At depths of 300 and 600 m, 38 kHz *TS* as a function of L_s was computed for the entire length range of captured fish from the model
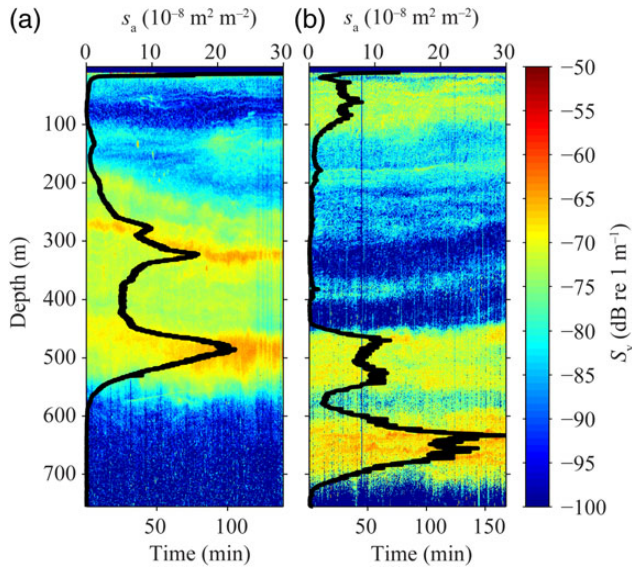
Figure 4. Echograms of volume backscattering strength (S_v) from the (a) CCE station (after dawn during second trawl), and (b) NPSG station (before sunset during first trawl). Profiles of the mean area backscattering coefficient (s_a) are shown as black lines. Both panels include a small portion of the DVM.

species. *TS* is not a linear function of L_s [i.e. $TS = m\log(L_s) + b$] for any of the three species (Figure 6). At 300 m depth, only the smallest *S. leucopsarus* (L_s 15−17 mm) and *D. theta* (L_s 10−13 mm) are resonant. However, these juvenile lanternfish have similar *TS* to adult *D. theta*, and a *TS* over 10 dB greater than the largest *S. leucopsarus* and *L. stilbius*. At 600 m depth, larger *D. theta* (L_s 12−18 mm) are resonant, as are *S. leucopsarus* of 17−39 mm L_s. This broad length range of *S. leucopsarus* resonates because their ESR remains almost constant as the fish grow and their swimbladder regresses (Figure 2).

Because the W_w of the smallest fish is almost three orders-of-magnitude below that of the largest, and because the *TS* of small *D. theta* and *S. leucopsarus* is similar to or greater than the *TS* of the largest fish, weight-specific backscattering decreases by over 20 dB for *D. theta* and *S. leucopsarus* as L_s increases from 10−60 mm. *Leuroglossus stilbius* shows a non-linear increase in weight-specific backscattering with L_s due to increasing cylindrical body radius relative to the acoustic wavelength combined with decreasing body density (Figure 6b).

Scattering from a population

Backscattering from the entire length distribution of each model species was normalized for relative abundance and summed for depths of 300 and 600 m (Figure 7). In all three species, abundance is dominated by small fish of L_s < 25 mm. However, most biomass is in individuals of L_s > 40 mm. The three modelled species differed in their backscattering cumulative distribution functions (CDF). In *D. theta*, 45% of the backscattering at 300 m depth is contributed by fish of L_s < 25 mm. However, at 600 m, *D. theta* of L_s < 25 mm comprise more than 70% of the total species backscattering due to the increased number of resonant fish. For *S. leucopsarus*, in which adults do not possess gas-filled swimbladders, ∼90% of the
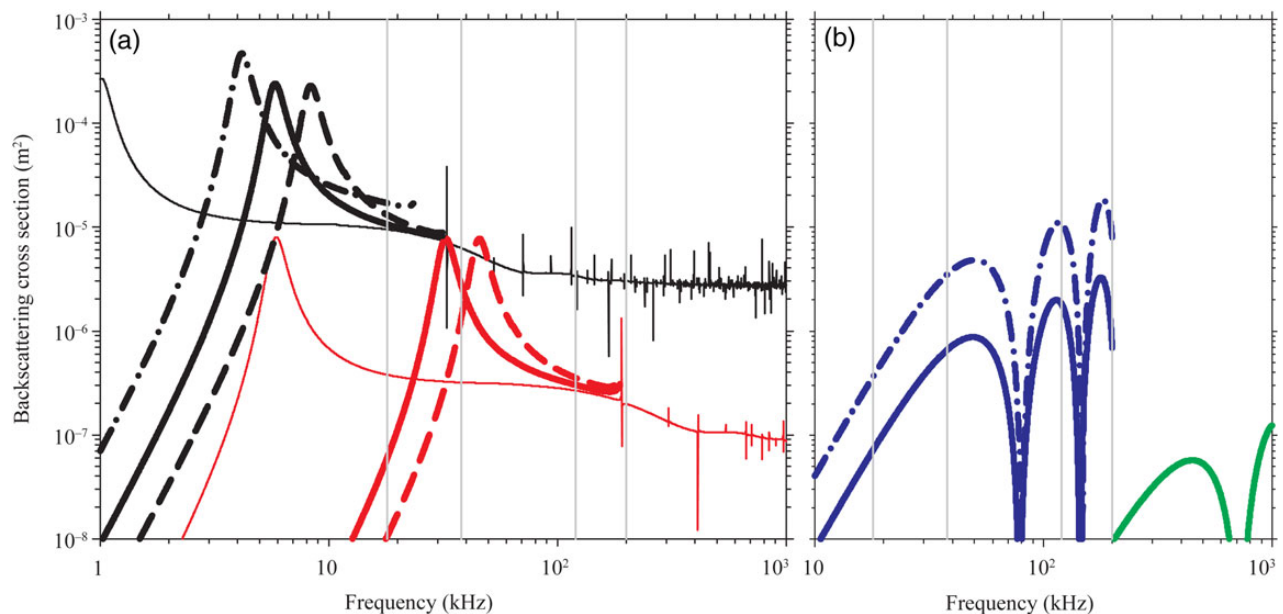
Figure 5. Modelled backscattering cross section (σ_{bs}) frequency spectra for (a) *D. theta*, and (b) *L. stilbius*. The smallest (L_s = 11 mm) and largest (L_s = 75 mm) *D. theta* are shown as red and black lines, respectively. σ_{bs} for the smallest (L_s = 16 mm) and largest (L_s = 84 mm) *L. stilbius* are shown as green and blue lines, respectively. Thick solid and dashed lines correspond to 300 and 600 m depth, respectively, with measured body density. Dash-dot lines correspond to models run at 300 m depth with a typical epipelagic fish body density of 1.076 g ml^{-1}. Thin lines correspond to σ_{bs} modelled at the surface. Grey vertical lines indicate 18, 38, 120, and 200 kHz frequencies.

Table 1. Echo integration (201–750 m) of the echograms in Figure 4 (CCE and NPSG stations) using differing methods of estimating the mean TS and W_w (columns "TS" and "W_w").

	CCE						NPSG					
	TS (dB)	W_w (g)	$S_{a,1}$ (dB)	$S_{a,2}$ (dB)	A (ind. m^{-2})	B (g m^{-2})	TS (dB)	W_w (g)	$S_{a,1}$ (dB)	$S_{a,2}$ (dB)	A (ind. m^{-2})	B (g m^{-2})
Trawl	–	0.8	–	–	5.8	4.9	–	0.2	–	–	6.5	1.3
TS_{300}	−59	0.8	−48	−49	22.1	18.4	−57	0.2	−61	−46	14.0	2.7
TS_{600}	−55	0.8	−48	−49	9.5	7.1	−54	0.2	−61	−46	7.7	1.5
Split	−59, −55	0.8	−48	−49	16.6	13.8	−57, −54	0.2	−61	−46	7.9	1.5
TS_{dom}	−61	2.5	−48	−49	40.6	102.0	−86	0.3	−61	−46	11 365	3 078
TS_{large}	−60	3.6	−48	−49	31.4	112.5	−59	0.9	−61	−46	24.7	22.4
TS_I	−60.6	1.0	−48	−49	34.7	35.5	−60.6	1.0	−61	−46	32.2	33.0
Trawl-CE	–	3.1	–	–	8.9	27.7	–	–	–	–	8.2	4.5
Split-CE	−59, −56	3.1	−48	−49	17.6	55.0	−57, −55	0.6	−61	−46	8.4	4.7

Columns "$S_{a,1}$" and "$S_{a,2}$" are the mean area backscattering strength for the 201–450 and 451–750 m depth ranges, respectively. Columns "A" and "B" indicate integrated acoustic abundance and biomass, respectively. Trawl abundance and biomass estimates are shown for comparison (row "Trawl"). Subsequent rows are: TS calculated at 300 m depth ("TS_{300}"), 600 m depth ("TS_{600}"), "Split" (TS_{300} used for depths 201–450 m and TS_{600} for depths 451–750 m), TS of the dominant species by biomass at 300 m depth ("TS_{dom}"; *S. leucopsarus* and *C. atraria* in the CCE and NPSG stations, respectively), TS of fish with $L_s > 40$ at 300 m depth ("TS_{large}"), abundance and biomass calculated using the assumed average TS and weight-specific scattering (30.7 dB kg^{-1}) from Irigoien *et al.* (2014; "TS_I"), trawl estimates made with the assumption of differential capture efficiency ("Trawl-CE"), and TS estimated using the "split" depth stratification and the differential capture efficiency assumption ("Split-CE").

species backscattering comes from individuals of $L_s < 25$ mm at both 300 and 600 m depth. In contrast, 90% of the population backscattering from *L. stilbius* comes from large fish of $L_s > 40$ mm, as does 60% of the biomass but only 10% of the abundance (Figure 7).

The effect of the differential capture efficiency assumption was to shift all abundance, biomass, and backscattering distributions towards larger fish (Figure 7). However, even with the differential capture efficiency assumption applied, abundance remains dominated by fish of $L_s < 25$ mm and biomass is still dominated by fish of $L_s > 40$ mm for all three model species (Figure 7).

Community backscattering

The CCE and NPSG stations had similar mesopelagic fish abundance and W_w range, but the CCE station had a greater proportion of large fish than the NPSG station (Figure 3; chiefly large lanternfish and dragonfish). Abundance at both stations was dominated by small fish of $L_s < 30$ mm, but these fish contributed only 6 and 25% of the biomass at the CCE and NPSG stations, respectively. Eighty per cent of the modelled backscattering at 300 m depth, and ~90% of the backscattering at 600 m, was from these small fish of $L_s < 30$ mm (Figure 8).

The same assumption of length-dependent capture efficiency used for the model species was applied to the catch from each station, shifting all distributions towards larger fish with the greatest effect on biomass. Under this assumption, more than half of the biomass was from fish of $L_s > 100$ mm; however, most of the abundance and backscattering was from fish of $L_s < 30$ mm (Figure 8).

The distribution of individual TS as a function of L_s at the two stations was similar, in that the small L_s fish that comprise most of the abundance and backscattering had a ~60 dB range in modelled TS (Figure 9). Fish with and without inflated swimbladders formed distinct groups separated by a 10–30 dB gap. The two groups converge with increasing L_s.

Estimation of abundance and biomass

Differing assumptions of depth, size, gear bias, and the degree that the dominant species is representative of the local fish community affect the estimates of TS and W_w and thus abundance and biomass by over 1 order of magnitude at the CCE station and over

3 orders of magnitude at the NPSG station (Table 1). The use of TS modelled at 600 m depth produces estimates of abundance and biomass close to the trawl estimates for both the CCE and NPSG stations. However, this is not a like-to-like comparison due to L_s-dependent avoidance of the net and because the entire DSL is shallower than 600 m in the CCE echogram (Figure 4). The use of depth-stratified TS estimates and the differential capture efficiency assumption for the trawl catch produced acoustic and trawl estimates of abundance and biomass within a factor of two at both stations. TS calculated from fish of $L_s > 40$ mm (as would be expected if TS is estimated from the catch of a large commercial trawl) and the mean TS of the dominant species (by biomass) both produce high estimates of abundance and biomass (Table 1).

Discussion

Our results clearly show that daytime acoustic estimates of mesopelagic fish biomass at 38 kHz are complicated by the small physical size of the fauna, mixed aggregations, swimbladder regression, resonance, effects of depth, ontogenetic decreases in fish body density, non-linear conversion of scattering strength to weight, and biases of the gear used for ground-truthing, as detailed below. Differing assumptions regarding depth, size distribution, and dominant species produce daytime acoustic biomass estimates spanning three orders of magnitude (Table 1). Additional complexity is introduced by DVM, which we do not consider here. Note that day–night differences in column scattering may not be large, even in the presence of resonance at depth. At the two stations considered here, trawling found ~20% of the overall mesopelagic fish abundance in the epipelagic at night (Davison *et al.*, 2013).

Length dependence of backscattering

For relatively large "typical" fish, TS increases with L_s in a linear fashion [$TS = m\log(L_s) + b$; Simmonds and MacLennan, 2005]. However, due to decreasing body density, swimbladder resonance, and ontogenetic changes in swimbladder inflation, TS does not increase linearly with increasing L_s for mesopelagic fish (Figure 6a). Fish species with regressing swimbladders may be resonant over a wide range of L_s, and as gas is lost completely, there is a sudden decrease in TS (~30 dB for *S. leucopsarus*) over the course of a few
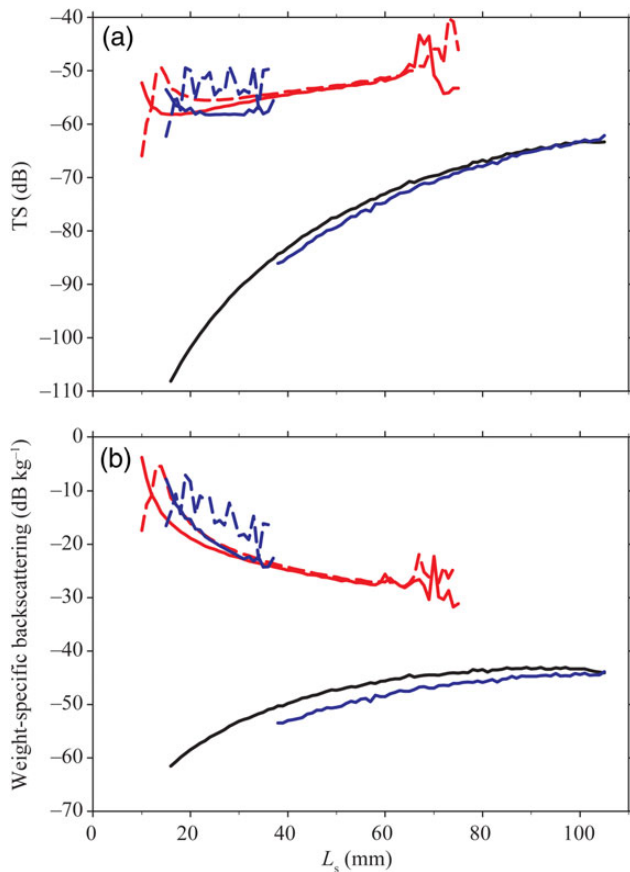
Figure 6. Backscattering from the L_s range of the three model species expressed as (a) *TS*, and (b) weight-specific backscattering. *Leuroglossus stilbius* is shown as black lines, *S. leucopsarus* as blue lines, and *D. theta* as red lines. Solid and dashed lines correspond to 300 and 600 m depths, respectively.

millimetres of growth (Figure 6a). The *TS* of mesopelagic fish in both ecosystems examined here spanned 60 dB, and is not easily described by a continuous relationship (Figure 9). Fish of L_s 10–400 mm may have a modelled $TS = -55$ dB, or a *TS* that is very different from that value (Figure 9). The depth-dependence of resonance frequency (Figure 5) adds further complexity to the estimation of *TS*. A change in depth less than the daily vertical movement of these fish can result in a *TS* change of over 10 dB (Figures 5 and 6). Simple $TS(L_s)$ relationships are inappropriate for the small fish that comprise the 38 kHz DSL.

Weight-specific backscattering is not constant with growth, and the shape of the curve differs for the three model species here. Weight-specific backscattering decreases ∼30 dB with L_s for fish with a swimbladder, increases ∼20 dB with L_s for fish without a swimbladder, and is a discontinuous combination of the two curves with a ∼50 dB range for fish in which the swimbladder regresses (Figure 6b). This, in combination with a length distribution skewed towards small fish, requires that estimates of the mean W_w and σ_{bs} for acoustic surveys consider the entire size structure of the population. Small fish cannot be neglected, even if they do not contribute significantly to biomass. At a depth of 600 m, 80% or more of interspecies backscattering is from fish of $L_s < 30$ mm that comprise <25% of the biomass (Figure 8). This dominance of backscattering by small fish is accentuated at depth because resonant frequency increases with depth and a larger

proportion of the population becomes resonant. It is robust to an assumed reduction in capture efficiency with increasing L_s and to community differences between the CCE and NPSG (Figures 7 and 8).

Choice of frequency for echo integration

The selection of survey frequency is important for mesopelagic fish. The EK60 system used here has five standard frequencies (18, 38, 70, 120, and 200 kHz), although often only a subset of these is installed. Frequency-dependent considerations are absorption (depth penetration), resonance, and body size of the animals present. For the purpose of surveying mesopelagic fish with a hull-based EK60, frequencies ≥ 120 kHz do not reach the daytime depth of the DSL and are thus inappropriate. The lower frequencies (18 and 38 kHz) enjoy the advantages of depth-penetration and low backscattering from non-target zooplankton and micronekton, but suffer the disadvantages of swimbladder resonance and the virtual exclusion of fish without gas-filled swimbladders due to their low *TS* (Figures 5 and 6). Because a greater proportion of mesopelagic fish resonate at 18 kHz compared with 38, 18 kHz is a poorer choice for surveys than is 38 kHz. We chose 38 kHz over 70 kHz for our simple survey to maximize depth penetration and minimize the contribution to backscattering by zooplankton.

Multifrequency acoustic data may be used to identify types and sizes of acoustic targets and correct for the effects of resonance at a particular frequency (Greenlaw and Johnson, 1983; Lavery *et al.*, 2007). Care must be taken with the application of multiple-frequency techniques to the DSL. Due to beam-spreading and distance from the transducer from hull-based systems, multiple targets are often ensonified. The differing frequency responses of these targets often outnumber the frequencies available, and thus multiple solutions are possible (i.e. the problem is underdetermined). dB differencing filters can be used to further exclude non-target organisms by taking advantage of differences in frequency spectra between different sizes of targets, and between gas bubbles and fluid-filled objects (Figure 5; Davison *et al.*, 2015). However, two frequencies (e.g. 18 and 38 kHz) are not sufficient to establish the dominant size class of swimbladders present, due to the confounding presence of non-resonant fish. Even if the relative abundance of resonant fish can be established with confidence, it is decoupled from biomass because larger non-resonant fish dominate biomass (Figure 8). Thus, multifrequency data must be cautiously interpreted in association with ground-truthing data. If a deeply deployed instrument platform is available, multifrequency techniques become more practical, as does detection of single scatterers and *in situ TS* measurements (Kloser *et al.*, 2013).

CCE and NPSG stations

Abundance of fish at the CCE and NPSG stations was similar (CCE:NPSG ratio = 0.9), but biomass differed (CCE:NPSG ratio = 3.8; Table 1). Trawl-based biomass estimates at these stations were similar to the published trawl-based estimates for those water masses (3.6 and 2.0 g m^{-2}, respectively; Gjosaeter and Kawaguchi, 1980). The two stations differed in that the CCE had more large fish and fewer very small fish than did the NPSG. Also, a greater proportion of fish at the NPSG station had gas-filled swimbladders (Figures 3 and 8). The DSL was ∼200 m deeper at the NPSG station than at the CCE station (Figure 4), perhaps due to a deeper oxygen minimum zone and increased light at depth in the NPSG (Garcia *et al.*, 2010; Koslow *et al.*, 2011). The two stations had similar measurements of column scattering 201–750 m (CCE:NPSG ratio = 1.1), but the NPSG station had greater
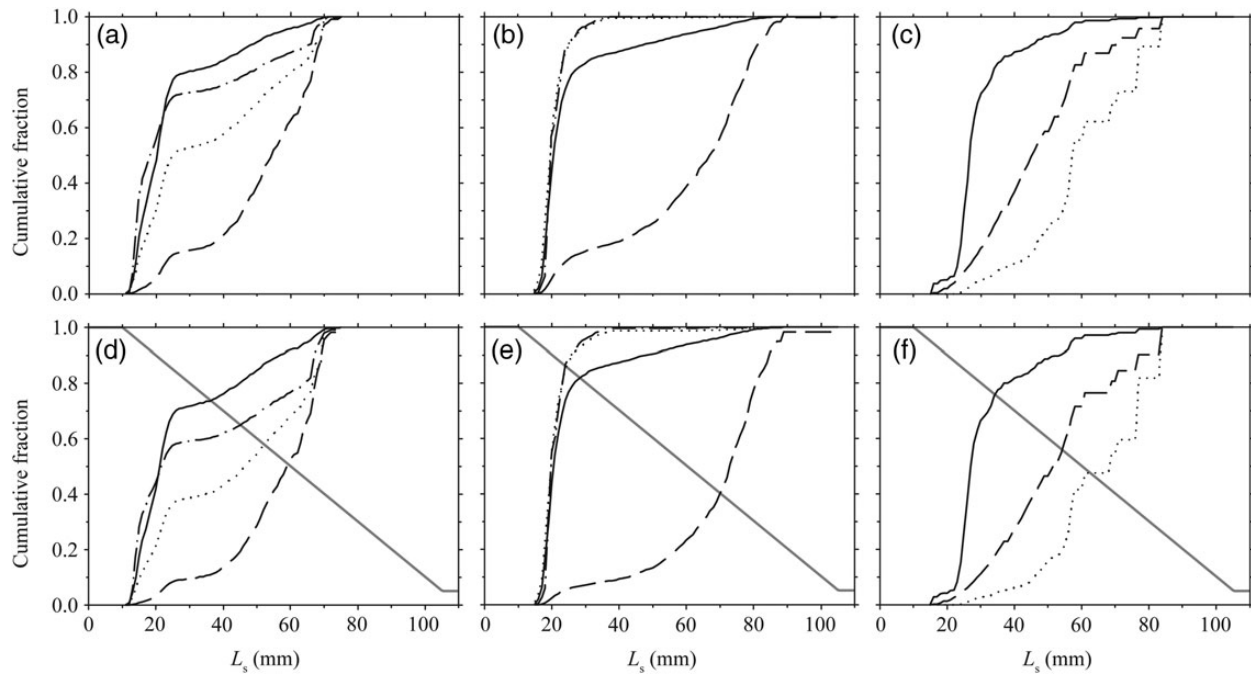
Figure 7. CDF of species abundance (solid line), biomass (dashed line), 300 m backscattering (dotted line), and 600 m backscattering (dash-dot line) for (a) *D. theta*, (b) *S. leucopsarus*, and (c) *L. stilbius*. Similar CDF assuming differential capture efficiency of the trawl by L_s are shown for (d) *D. theta*, (e) *S. leucopsarus*, and (f) *L. stilbius*. Assumed capture efficiency is shown as a thick grey line on the same *y*-axis, using the same scale as cumulative fraction.
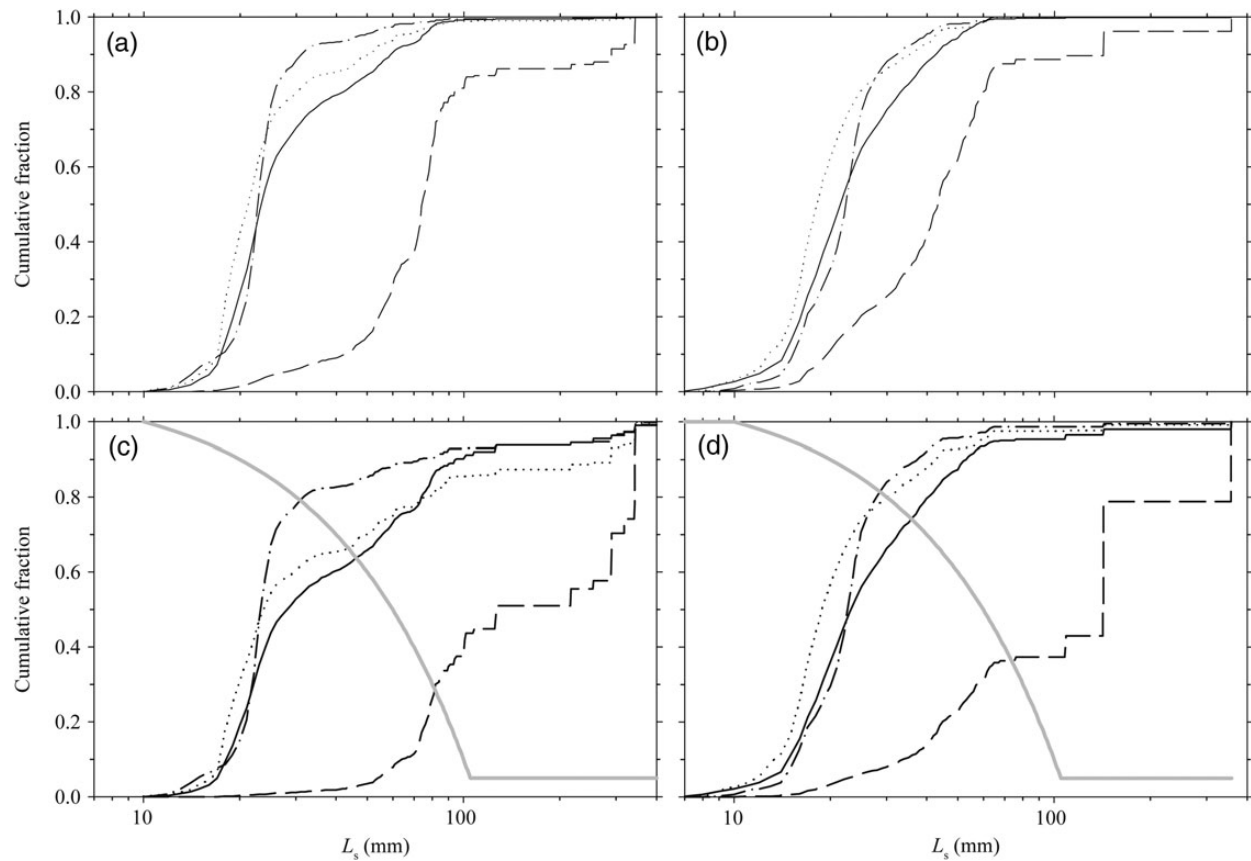
Figure 8. CDF of species abundance (solid line), biomass (dashed line), 300 m backscattering (dotted line), and 600 m backscattering (dash-dot line) for all fish from the (a) CCE station and (b) NPSG station. Similar CDF assuming differential capture efficiency of the trawl (by L_s) are shown for (c) the CCE station and (d) the NPSG station. Assumed capture efficiency is shown as a thick grey line on the same *y*-axis, using the same scale as cumulative fraction. Note the log scale of the *x*-axis.

abundance of potentially resonant small fish with inflated swimbladders (Figure 3). This indicates that more of the small fish at the NPSG station were non-resonant in either the geometric region (shallower than the resonant depth) or the Rayleigh region (deeper than the resonant depth) of their frequency spectra, or that there were differences between the two stations in swimbladder gas volume with respect to depth (i.e. constant mass vs. constant volume of swimbladder gas). Depth-stratified sampling is required to resolve which of these possibilities is true. Because *C. signata*, the numerically dominant fish at both stations, has an inflated swimbladder and is of resonant size, it is probably the single greatest contributor to the non-migratory 38 kHz DSL at both stations.

Acoustic estimates of biomass will be biased if the ground-truthing (trawl catch) is unevenly selective for species composition and size. This trawl selectivity bias will affect the derived mean *TS* and W_w used to convert the acoustic data to biomass, in addition to affecting the trawl estimate of biomass itself. The difference between the acoustic and trawl estimates is often attributed to
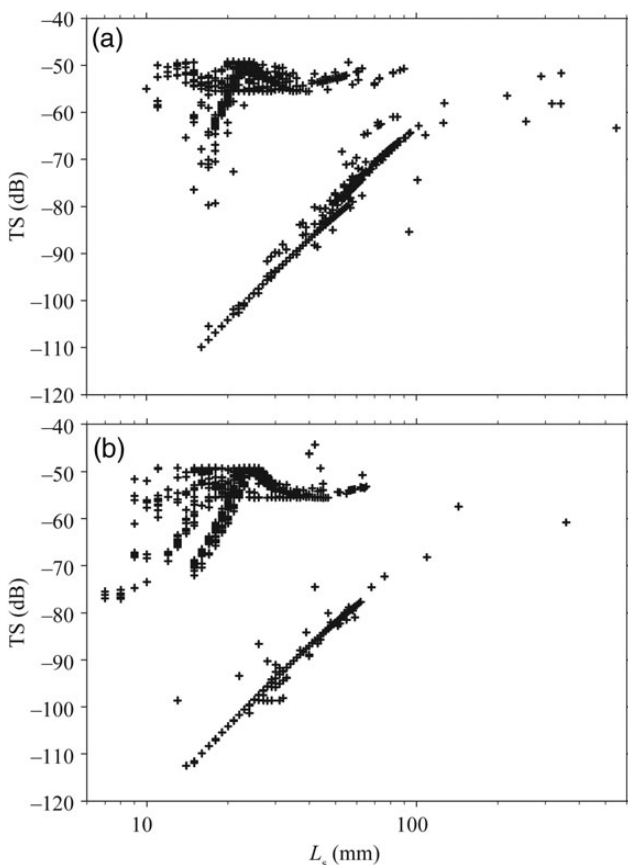
Figure 9. Modelled *TS* at 600 m depth (plus sign) of all individual fish of all species captured at the (a) CCE station, and (b) NPSG station.

capture efficiency. With a common assumption of capture efficiency, synoptic acoustic and trawl estimates of biomass should match, if other underlying assumptions are reasonable. Several methods of calculating the mean *TS* and W_w were applied to example daytime S_v echograms from the CCE and NPSG stations (Figure 4, Table 1). The mean modelled σ_{bs} of the trawl catches was approximately twice as high at an assumed depth of 600 m as at 300 m, producing lower biomass estimates (Table 1). Splitting the s_a depth vector into shallow and deep sections, and applying the corresponding mean *TS* produced intermediate (to TS_{300} and TS_{600}) abundance and biomass estimates. At the NPSG station, this "split" estimate was close to the TS_{600} estimate because there was very little backscattering in the depth range 200–450 m (Figure 4). Compared with the trawl catch, these "split" estimates correspond to L_s-independent capture efficiencies of ~35 and ~85% for the CCE and NPSG stations, respectively. The use of *TS* and W_w estimated from the largest fish (emulating the catch of a commercial trawl) or from the dominant species for biomass at the station produced clear overestimates of abundance and biomass. Irigoien *et al.* (2014) used a *TS* calculated from lanternfish of $L_s = 60$ mm in combination with a weight-specific backscattering estimate throughout their global study. These methods produce a biomass estimate similar to that of the trawl (with the differential capture efficiency assumption) at the CCE station, but at the NPSG station, the acoustic estimate exceeds that of the trawl by a factor of seven (Table 1). This, in combination with the areal preponderance of subtropical gyres in the global ocean, could explain the high global biomass estimates recently published by Irigoien *et al.* (2014). The most sophisticated *TS* estimate used here ("split-CE" method; Table 1) is similar to the "split" method, but assumed increasing ability of fish to avoid the MOHT with increasing L_s. This assumption increased trawl estimates of abundance, biomass, and mean W_w, but not mean *TS*. At the CCE station, acoustic abundance and biomass estimates were approximately twice as high as the (adjusted) trawl estimates, whereas at the NPSG station, the acoustic estimates were approximately equal to the trawl estimates. This disparity could be due to sampling variability by the MOHT, the dominance of biomass by species with regressed swimbladders in the CCE, the greater dominance of small fish in the NPSG, or differences between the two stations in the depth distribution of L_s and swimbladder inflation.

Ground-truthing

Trawling, in combination with acoustic forward modelling, is often used to "ground-truth" the species present, mean σ_{bs} and mean W_w. It must be emphasized to note that the mean σ_{bs} is not equivalent to the σ_{bs} of a fish with the mean W_w, and that the two quantities may differ by as much as two orders of magnitude (Table 2). These parameters must be re-evaluated at the same scale at which the community composition changes; vertically, horizontally, and temporally. Even in single-species aggregations or low-diversity mesopelagic

Table 2. Error resulting from the use of the *TS* of a fish with the mean W_w rather than the mean *TS* of the length distribution of the three model species.

Species	Mean W_w (g)	L_s of mean W_w (mm)	TS of mean W_w (dB)	Mean TS (dB)	Error factor
S. leucopsarus	0.46	36	−49.7	−54.8	0.3
D. theta	0.62	33.5	−54.7	−48.3	4.4
L. stilbius	0.18	30	−90.6	−68.2	175.0

"Error factor" is the ratio of echo integration biomass calculated with the *TS* of a fish with the mean W_w to that calculated from the mean *TS* of the population.

ecosystems, the distribution and relative abundance of fish of different lengths must be known for credible interpretation of backscattering. Unfortunately, most methods of ground-truthing are biased in their own sampling, and multiple methods may be required to aid the interpretation of acoustic data (McClatchie *et al.*, 2000).

Estimation of the mean σ_{bs} requires knowledge of gas content, gas volume, and body density of the fish present (for forward modelling) or *in situ* TS measurements. *In situ* TS measurements at DSL depths are problematic from hull-mounted transducers due to beam spreading. The large volumes of water ensonified at depth in combination with high abundances in the DSL provide few of the "single targets" required for *in situ* TS measurements. Thus, transducers mounted on platforms at depth are required for *in situ* TS measurements in the DSL (Kloser *et al.*, 2002).

The mean W_w estimates require physical sampling of the species and L_s distributions present (trawls) or *in situ* species identification and L_s measurements [cameras still require a measured $W_w(L_s)$ relationship]. The use of either cameras or trawls requires compensation for avoidance and escapement biases, which differ between the two instruments. The use of commercial-sized trawls for ground-truthing is inadequate because they have wide meshes that do not well retain the size class of fish that produces more than 80% of the backscattering. Even a constant 4-mm mesh can lose more than 60% of the fish of $L_s < 30$ mm through escapement (Gartner *et al.*, 1989). Moderate-size midwater trawls fitted with fine mesh can retain the small fish that provide much of the backscattering in the DSL, but have a poorly known avoidance bias. We used an L_s-dependent catch compensation assumption that is consistent with what is known about trawl avoidance, but is not empirically based. More data are required on length-dependent trawl avoidance.

Ground-truthing is also required to identify other taxa present in the DSL beside mesopelagic fish. Pteropods, siphonophores, and mesopelagic crustaceans (such as euphausiids) are all strong scatterers and co-occur with fish. All of these taxa may be locally abundant and dominate backscattering (Warren *et al.*, 2001; Lavery *et al.*, 2007).

Sources of error in forward modelling

Forward acoustic modelling of the catch from a trawl is complex, and relies on many assumed parameters. Some of these are estimates of material properties (sound speed, density, damping coefficient), others are simplifications of shape (swimbladder, body, internal structure), and some are behavioural or morphological (tilt angle, presence and volume of gas in the swimbladder). If the trawl is not depth-stratified, there is an implicit assumption that species and size (W_w, L_s) distributions are constant with depth. Confidence is gained in a model through independent *in situ* (Kloser *et al.*, 2013) or *ex situ* (Yasuma *et al.*, 2006) acoustic measurements with optical verification.

Our acoustic model of small mesopelagic fish is consistent with other models and *ex situ* measurements under similar conditions (depth, gas volume). However, it remains unclear how well these models perform at DSL depths. We assumed gas volumes sufficient for neutral buoyancy at all depths based upon observations of torpid, non-sinking mesopelagic fish at depth (Barham, 1971; Kaartvedt *et al.*, 2009) and unpublished observations of constant S_v in vertically migrating layers. This assumption needs to be tested, as some (larger) deep-living fish have been observed to be negatively buoyant (Kloser *et al.*, 2011). Fish of the same L_s and species can vary in their swimbladder inflation after capture at the

surface (Yasuma *et al.*, 2008; Davison, 2011a), but it is unknown if this is true at depth before handling. Gas volume measurements at the surface are problematic due to the differences between temperature and pressure at the surface and those at the depth where the animal was captured. Fish may resorb gas during the depth changes associated with capture, or gas may be lost during handling (Davison, 2011a). Additionally, it is unknown to what degree undisturbed fish allow the swimbladder gas to expand and compress with changes in depth, and the mechanisms may be complex (Love *et al.*, 2004). Thus, surface measurements of gas volume are inadequate for modelling purposes and *in situ* data are required for mesopelagic fish.

Tilt angle is of little importance to 38 kHz TS for mesopelagic fish with gas-filled swimbladders, but is crucial to the TS estimation of fish without inflated swimbladders (Yasuma *et al.*, 2010). Because tilt angle cannot be measured with nets, it must be established *in situ* for acoustic surveys in which the backscattering from fish without functional swimbladders is important. Visually verified *in situ* target strengths with stereo optical measures of tilt angle can provide this measurement (Kloser *et al.*, 2013).

Conclusions

The 38 kHz backscattering from mesopelagic fish is depth-sensitive and non-linear with respect to size, and can decrease with increasing fish length, as can weight-specific backscattering (Figures 5, 6, and 9). Populations and communities of mesopelagic fish have a size structure in which abundance is skewed towards the smallest fish and biomass towards the largest fish (Figures 3, 7, and 8). Thus, echograms of S_v reflect the distribution of the strongest scatterers (possibly the smallest fish), and not necessarily biomass. The fish that contribute the bulk of biomass are indirectly estimated from catch ratios through the use of the mean W_w and mean σ_{bs}. It is incorrect to use the σ_{bs} of a fish with the mean W_w for echo integration (error factor 0.3–175), as it is not the same as the mean σ_{bs} of the population, which is required to estimate abundance from acoustic data (Table 2).

The chief advantages of mesopelagic acoustic data over trawl surveys are fine horizontal and vertical spatial scale, and the lack of avoidance and escapement biases. However, fine-scale interpretation of mesopelagic acoustic data is not possible without concurrent ground-truthing at the horizontal and vertical scale in which the "heavy fish" vary in proportion to the "backscattering fish". This proportion is likely to change across fronts, eddies, productivity gradients, bottom topography, depth, season, and diel cycle. Ground-truthing itself is fraught with difficulties such as gear bias (depth of occurrence, avoidance, attraction, and escapement), the unsuitability of nets to capture siphonophores, the difficulty of identifying single targets at DSL depths, the inability to reach the DSL with hull-based high frequency sonar, and unknown acoustic properties of mesopelagic taxa.

Credible estimates of mesopelagic fish biomass must consider the taxa present, the community size structure, and the depth-sensitivity of acoustic properties. A definitive estimate of mesopelagic fish biomass would likely require depth-stratified trawls with a fine mesh, forward acoustic modelling of the entire catch, multifrequency acoustic data from a deeply deployed platform, an optical survey for siphonophores, measurement of length-dependent avoidance and escapement by fish of the trawl, dissections of fish for swimbladder inflation, measurements of fish body density, and support of modelling theory with paired optical identification and *in situ* TS measurements. Where these data are not available, acoustic results must be

interpreted with caution. However, all is not lost. Depth-stratified ground-truthing and future work globally on net avoidance, acoustic properties of species, and forward modelling theory will support increasingly credible acoustic estimates of DSL biomass. This would lead to better monitoring, modelling and predictive capability of ecosystem dynamics in the open ocean (Handegard *et al.*, 2013).

References

Anderson, V. C. 1950. Sound scattering from a fluid sphere. Journal of the Acoustical Society of America, 22: 426–431.

Barham, E. G. 1963. Siphonophores and the deep scattering layer. Science, 140: 826–828.

Barham, E. G. 1971. Deep-sea fishes: lethargy and vertical orientation. *In* Proceedings of an International Symposium on Biological Sound Scattering in the Ocean, pp. 100–118. Ed. by G. B. Farquhar. US Government Printing Office, Washington, DC.

Butler, J. L., and Pearcy, W. G. 1972. Swimbladder morphology and specific gravity of myctophids off Oregon. Journal of the Fisheries Research Board of Canada, 29: 1145–1150.

Clay, C. S., and Horne, J. K. 1994. Acoustic models of fish—the Atlantic cod (*Gadus morhua*). Journal of the Acoustical Society of America, 96: 1661–1668.

Davison, P. 2011a. The buoyancy of mesopelagic fishes from the northeast Pacific Ocean and its implications for acoustic backscatter. ICES Journal of Marine Science, 68: 2064–2074.

Davison, P. 2011b. The export of carbon mediated by mesopelagic fishes in the northeast Pacific Ocean. Scripps Institution of Oceanography, p. 149. University of California, San Diego, La Jolla.

Davison, P., Lara-Lopez, A., and Koslow, J. A. 2015. Mesopelagic fish biomass in the southern California Current ecosystem. Deep Sea Research II, 112: 129–142.

Davison, P. C., Checkley, D. M., Koslow, J. A., and Barlow, J. 2013. Carbon export mediated by mesopelagic fishes in the northeast Pacific Ocean. Progress in Oceanography, 116: 14–30.

De Robertis, A., and Higginbottom, I. 2007. A post-processing technique to estimate the signal-to-noise ratio and remove echosounder background noise. ICES Journal of Marine Science, 64: 1282–1291.

Foote, K. G., Knudsen, H. P., Vestnes, G., MacLennan, D. N., and Simmonds, E. J. 1987. Calibration of acoustic instruments for fish density estimation: a practical guide. ICES Cooperative Research Report, 144.

Garcia, H. E., Locarnini, R. A., Boyer, T. P., Antonov, J. I., Baranova, H. A., Zweng, M. M., and Johnson, D. R. 2010. World Ocean Atlas 2009, Volume 3: Dissolved Oxygen, Apparent Oxygen Utilization, and Oxygen Saturation. US Government Printing Office, Washington, DC.

Gartner, J. V., Conley, W. J., and Hopkins, T. L. 1989. Escapement by fishes from midwater trawls—a case study using lanternfishes (Pisces: Myctophidae). Fishery Bulletin, 87: 213–222.

Gartner, J. V., Crabtree, R. E., and Sulak, K. J. 1997. Feeding at depth. *In* Deep-Sea Fishes, pp. 115–193. Ed. by D. J. Randall, and A. P. Farrell. Academic Press, San Diego.

Gjosaeter, J., and Kawaguchi, K. 1980. A review of the world resources of mesopelagic fish. FAO Fisheries Technical Paper, 193: 1–151.

Godo, O. R., Patel, R., and Pedersen, G. 2009. Diel migration and swimbladder resonance of small fish: some implications for analyses of multifrequency echo data. ICES Journal of Marine Science, 66: 1143–1148.

Greenlaw, C. F., and Johnson, R. K. 1983. Multiple frequency acoustical estimation. Biological Oceanography, 2: 227–252.

Handegard, N. O., du Buisson, L., Brehmer, P., Chalmers, S. J., De Robertis, A., Huse, G., Kloser, R., *et al.* 2013. Towards an acoustic-based coupled observation and modelling system for monitoring and predicting ecosystem dynamics of the open ocean. Fish and Fisheries, 14: 605–615.

Hersey, J. B., Backus, R. H., and Hellwig, J. 1962. Sound-scattering spectra of deep scattering layers in the western North Atlantic Ocean. Deep Sea Research, 8: 196–210.

Irigoien, X., Klevjer, T. A., Rostad, A., Martinez, U., Boyra, G., Acuna, J. L., Bode, A., *et al.* 2014. Large mesopelagic fishes biomass and trophic efficiency in the open ocean. Nature Communications, 5: 3271.

Isaacs, J. D., and Kidd, L. W. 1953. Isaacs-Kidd midwater trawl final report. Scripps Institution of Oceanography Oceanographic Equipment Report, 1: 1–21.

Itaya, K., Fujimori, Y., Shimizu, S., Komatsu, T., and Miura, T. 2007. Effect of towing speed and net mouth size on catch efficiency in framed midwater trawls. Fisheries Science, 73: 1007–1016.

Johnson, R. K. 1977. Sound scattering from a fluid sphere revisited. Journal of the Acoustical Society of America, 61: 375–377.

Kaartvedt, S., Rostad, A., Klevjer, T. A., and Staby, A. 2009. Use of bottom-mounted echo sounders in exploring behavior of mesopelagic fishes. Marine Ecology Progress Series, 395: 109–118.

Kaartvedt, S., Staby, A., and Aksnes, D. L. 2012. Efficient trawl avoidance by mesopelagic fishes causes large underestimation of their biomass. Marine Ecology Progress Series, 456: 1–6.

Kloser, R. J., Macaulay, G. J., Ryan, T. E., and Lewis, M. 2013. Identification and target strength of orange roughy (*Hoplostethus atlanticus*) measured *in situ*. Journal of the Acoustical Society of America, 134: 97–108.

Kloser, R. J., Ryan, T. E., Macaulay, G. J., and Lewis, M. E. 2011. *In situ* measurements of target strength with optical and model verification: a case study for blue grenadier, *Macruronus novaezelandiae*. ICES Journal of Marine Science, 68: 1986–1995.

Kloser, R. J., Ryan, T., Sakov, P., Williams, A., and Koslow, J. A. 2002. Species identification in deep water using multiple acoustic frequencies. Canadian Journal of Fisheries and Aquatic Sciences, 59: 1065–1077.

Kloser, R. J., Ryan, T. E., Young, J. W., and Lewis, M. E. 2009. Acoustic observations of micronekton fish on the scale of an ocean basin: potential and challenges. ICES Journal of Marine Science, 66: 998–1006.

Koslow, J. A., Goericke, R., Lara-Lopez, A., and Watson, W. 2011. Impact of declining intermediate-water oxygen on deepwater fishes in the California Current. Marine Ecology Progress Series, 436: 207–218.

Koslow, J. A., Kloser, R. J., and Williams, A. 1997. Pelagic biomass and community structure over the mid-continental slope off southeastern Australia based upon acoustic and midwater trawl sampling. Marine Ecology Progress Series, 146: 21–35.

Lavery, A. C., Wiebe, P. H., Stanton, T. K., Lawson, G. L., Benfield, M. C., and Copley, N. 2007. Determining dominant scatterers of sound in

mixed zooplankton populations. Journal of the Acoustical Society of America, 122: 3304–3326.

Love, R. H., Fisher, R. A., Wilson, M. A., and Nero, R. W. 2004. Unusual swimbladder behavior of fish in the Cariaco Trench. Deep Sea Research, 51: 1–16.

Mackenzie, K. V. 1981. Nine-term equation for sound speed in the oceans. Journal of the Acoustical Society of America, 70: 807–812.

MacLennan, D. N., Fernandes, P. G., and Dalen, J. 2002. A consistent approach to definitions and symbols in fisheries acoustics. ICES Journal of Marine Science, 59: 365–369.

Mann, K. H. 1984. Fish production in open ocean ecosystems. *In* Flows of Energy and Materials in Marine Ecosystems, pp. 435–458. Ed. by M. J. R. Fasham. Plenum Press, New York.

McClatchie, S., Thorne, R. E., Grimes, P., and Hanchet, S. 2000. Ground truth and target identification for fisheries acoustics. Fisheries Research, 47: 173–191.

Millero, F. J., Chen, C. T., Schleicher, K., and Bradshaw, A. 1980. A new high pressure equation of state for seawater. Deep Sea Research, 27: 255–264.

Murphy, G. I., and Clutter, R. I. 1972. Sampling anchovy larvae with a plankton purse seine. Fishery Bulletin, 70: 789–798.

Oozeki, Y., Hu, F. X., Kubota, H., Sugisaki, H., and Kimura, R. 2004. Newly designed quantitative frame trawl for sampling larval and juvenile pelagic fish. Fisheries Science, 70: 223–232.

Pakhomov, E. A., Perissinotto, R., and McQuaid, C. D. 1996. Prey composition and daily rations of myctophid fishes in the Southern Ocean. Marine Ecology Progress Series, 134: 1–14.

Robison, B. H., Reisenbichler, K. R., Sherlock, R. E., Silguero, J. M. B., and Chavez, F. P. 1998. Seasonal abundance of the siphonophore, *Nanomia bijuga*, in Monterey Bay. Deep Sea Research II, 45: 1741–1751.

Saenger, R. A. 1989. Bivariate normal swimbladder size allometry models and allometric exponents for 38 mesopelagic swimbladdered fish species commonly found in the north Sargasso Sea. Canadian Journal of Fisheries and Aquatic Sciences, 46: 1986–2002.

Simmonds, J., and MacLennan, D. 2005. Fisheries Acoustics: Theory and Practice. Blackwell Science, Oxford.

Stanton, T. K. 1988. Sound scattering by cylinders of finite length. I. Fluid cylinders. Journal of the Acoustical Society of America, 83: 55–63.

Warren, J. D., Stanton, T. K., Benfield, M. C., Wiebe, P. H., Chu, D., and Sutor, M. 2001. *In situ* measurements of acoustic target strengths of gas-bearing siphonophores. ICES Journal of Marine Science, 58: 740–749.

Yamamura, O., Suntsov, A. V., and Yasuma, H. 2010. Third micronekton inter-calibration experiment, MIE-3. *In* Report of the Advisory Panel on Micronekton Sampling Inter-calibration Experiment, pp. 59–65. Ed. by E. A. Pakhomov, and O. Yamamura. North Pacific Marine Science Organization (PICES), Sidney.

Yasuma, H., Sawada, K., Miyashita, K., and Aoki, I. 2008. Swimbladder morphology and target strength of myctophid fishes in the northwestern Pacific. Journal of the Marine Acoustics Society of Japan, 35: 17–28.

Yasuma, H., Sawada, K., Takao, Y., Miyashita, K., and Aoki, I. 2010. Swimbladder condition and target strength of myctophid fish in the temperate zone of the Northwest Pacific. ICES Journal of Marine Science, 67: 135–144.

Yasuma, H., Takao, Y., Sawada, K., Miyashita, K., and Aoki, I. 2006. Target strength of the lanternfish, *Stenobrachius leucopsarus* (family Myctophidae), a fish without an airbladder, measured in the Bering Sea. ICES Journal of Marine Science, 63: 683–692.

Yasuma, H., and Yamamura, O. 2010. Comparison between acoustic estimates. *In* Report of the Advisory Panel on Micronekton Sampling Inter-calibration Experiment, pp. 51–57. Ed. by E. A. Pakhomov, and O. Yamamura. North Pacific Marine Science Organization (PICES), Sidney.

Handling editor: Richard O'Driscoll